Strong magnetoresistance of disordered graphene

P. S. Alekseev,[1] A. P. Dmitriev,[1] I. V. Gornyi,[1,2] and V. Yu. Kachorovskii[1]

[1]*A.F. Ioffe Physico-Technical Institute, 194021 St. Petersburg, Russia*
[2]*Institut für Nanotechnologie, Karlsruhe Institute of Technology, D-76021 Karlsruhe, Germany*

We study theoretically magnetoresistance (MR) of graphene with different types of disorder. For short-range disorder, the key parameter determining magnetotransport properties—a product of the cyclotron frequency and scattering time—depends in graphene not only on magnetic field H but also on the electron energy ε. As a result, a strong, square root in H, MR arises already within the Drude-Boltzmann approach. The MR is particularly pronounced near the Dirac point. Furthermore, for the same reason, "quantum" (separated Landau levels) and "classical" (overlapping Landau levels) regimes may coexist in the same sample at fixed H. We calculate the conductivity tensor within the self-consistent Born approximation for the case of relatively high temperature, when Shubnikov-de Haas oscillations are suppressed by thermal averaging. We predict a square-root MR both at very low and at very high H : $[\varrho_{xx}(H) - \varrho_{xx}(0)]/\varrho_{xx}(0) \approx C\sqrt{H}$, where C is a temperature-dependent factor, different in the low- and strong-field limits and containing both "quantum" and "classical" contributions. We also find a nonmonotonic dependence of the Hall coefficient both on magnetic field and on the electron concentration. In the case of screened charged impurities, we predict a strong temperature-independent MR near the Dirac point. Furthermore, we discuss the competition between disorder- and collision-dominated mechanisms of the MR. In particular, we find that the square-root MR is always established for graphene with charged impurities in a generic gated setup at low temperature.

I. INTRODUCTION

Study of magnetotransport in low-dimensional systems is a powerful tool to probe the nature of disorder and extract information about localization phenomena. In particular, measurements of magnetoresistance (MR) of two-dimensional (2D) electron gas in conventional semiconductors, like GaAs, allowed one to identify a variety of different regimes, such as Drude-Boltzmann quasiclassical transport, weak localization regime, and the quantum Hall effect (see Refs. 1 and 2 for review).

One of the simplest theoretical approaches to the problem, the so-called self-consistent Born approximation (SCBA), was developed in Refs. 3–6 for 2D electrons with quadratic spectrum mostly for the case of the short-range disorder. The SCBA approach ignores localization effects. This implies that the relevant energy scale (the maximum of the chemical potential μ and temperature T) is large compared to the inverse transport scattering time $\tau_{\rm tr}$, which coincides with the quantum scattering time τ_q for the short-range disorder. The key parameter of SCBA is $\omega_c \tau_q$, where ω_c is the cyclotron frequency. For weak magnetic fields, $\omega_c \tau_q \ll 1$, calculations[6] reproduce the semiclassical Drude-Boltzmann result. In the opposite limit, $\omega_c \tau_q \gg 1$, the semiclassical approach fails, and the conductivity is given by a sum of contributions coming from the well-separated Landau levels (LLs).[3–6]

Magnetotransport in graphene was studied theoretically in Refs. 7–14. In Refs. 7 and 8 a general expression for the SCBA conductivity tensor of graphene with short-range disorder was derived and analyzed in detail for the case of well-separated LLs. Other types of disorder were also discussed,[9–11] including disorder potentials having special types of symmetries.[12] In the collision-dominated regime (when the rate of inelastic collisions due to the electron-electron interaction exceeds the impurity-induced scattering

rate), the MR of graphene at the Dirac point was calculated in Ref. 13 within the Boltzmann-equation framework by using the relativistic hydrodynamic approach. In Ref. 14, a T-dependent interaction-induced contribution to the MR (on top of a substantial positive T-independent MR) was observed experimentally and analyzed theoretically.

A specific property of graphene compared to conventional 2D semiconductors is the linear energy dispersion of the carriers,

$$\varepsilon_{\rm k} = \pm v\hbar k, \tag{1}$$

resulting in the density of states, which increases away from the Dirac point:

$$\nu_0(\varepsilon) = \frac{N|\varepsilon|}{2\pi v^2 \hbar^2}. \tag{2}$$

Here $v = 10^8$ cm/c is the Fermi velocity, ε is the energy counted from the Dirac point and $N = 2 \times 2 = 4$ is the spin-valley degeneracy. Corresponding wave functions are given by $\exp(i\mathbf{k}\mathbf{r})|\chi_\varphi\rangle$, where $|\chi_\varphi\rangle$ is the spinor with the components $(e^{-i\varphi/2}, \pm e^{i\varphi/2})/\sqrt{2}$, and φ denotes the polar angle of the momentum $\mathbf{k}$.

Important consequence of the linear dispersion of graphene is that the cyclotron frequency turns out to be energy dependent:[15]

$$\omega_c(\varepsilon) = \frac{eH}{cm(\varepsilon)} = \frac{\hbar \Omega^2}{\varepsilon}, \quad \text{for} \quad \varepsilon \gg \Omega. \tag{3}$$

Here H is the magnetic field and $m(\varepsilon) = \varepsilon/v^2$ is the energy-dependent cyclotron mass. The frequency,

$$\Omega = \frac{v}{l_H}, \tag{4}$$

is proportional to the distance between the lowest LLs [see Eq. (24) below], where $l_H = \sqrt{c\hbar/eH}$ is the magnetic length.

Another consequence is the energy dependence of quantum and momentum relaxation times for the short-range scattering potential. Here we by definition assume that the random potential is a short-range one if its radius R satisfies the following inequalities,

$$a \ll R \ll \lambda, \qquad (5)$$

where a is the lattice constant and λ is the electron wavelength (this definition is different from one chosen in Refs. [16] and [17]). Such a potential does not mix valleys and can be written as[7,16]

$$\hat{V}(\mathbf{r}) = V(\mathbf{r}) \begin{pmatrix} 1 & 0 \\ 0 & 1 \end{pmatrix}, \quad V(\mathbf{r}) = u_0 \sum_i \delta(\mathbf{r} - \mathbf{r}_i), \qquad (6)$$

where summation is taken over the impurity positions. The correlation function of $V(\mathbf{r})$ is given by $\langle V(\mathbf{r})V(\mathbf{r}') \rangle = \kappa \delta(\mathbf{r} - \mathbf{r}')$, where $\kappa = n_{\mathrm{imp}} u_0^2$ and n_{imp} is the impurity concentration. Calculating by golden rule the quantum and transport scattering times we find that they are different and both energy dependent:[7,15]

$$\tau_q(\varepsilon) = \frac{\gamma \hbar}{|\varepsilon|}, \quad \tau_{tr}(\varepsilon) = 2\tau_q(\varepsilon), \qquad (7)$$

where $\gamma = 2\hbar^2 v^2/\kappa$. The difference between τ_{tr} and τ_q is due to weak anisotropy of the scattering arising from the spinor nature of the wave functions. Indeed, the squared scattering matrix element, $|U_{\mathbf{k'k}}|^2$ is proportional to $|\langle \chi_{\varphi'}|\chi_\varphi \rangle|^2$ and, therefore, depends on the scattering angle $\varphi - \varphi'$. Below we assume that $\gamma \gg 1$ and, consequently, $\varepsilon \tau_q(\varepsilon)/\hbar \gg 1$. The latter inequality allows us to neglect localization effects. We also assume that disorder does not affect density of states. This condition is also satisfied for large γ, with an exception for exponentially small energies,[17] $\varepsilon \sim \Delta \, e^{-\pi\gamma/2}$ (Δ is the bandwidth of graphene), which are irrelevant for this paper. Under such assumptions the conductivity in zero magnetic field is given by the Drude formula:

$$\sigma_{xx}^D = \sigma_0 = \frac{2e^2 \gamma}{\pi \hbar}, \quad \text{for} \quad H = 0. \qquad (8)$$

We see that both ω_c and τ_q are energy dependent and, therefore, the parameter,

$$x = \omega_c \tau_q = \frac{\varepsilon_*^2}{\varepsilon^2}, \qquad (9)$$

can be small or large at the same sample for different ε. Here we used Eqs. (3) and (7) and introduced the energy,

$$\varepsilon_* = \hbar \Omega \sqrt{\gamma} \gg \hbar \Omega, \qquad (10)$$

which scales as a square root of the magnetic field:

$$\varepsilon_* \propto \sqrt{H}. \qquad (11)$$

As seen from Eq. (9), at sufficiently high T the temperature window might include both the "quantum" ($x > 1$) and the "classical" ($x < 1$) regions, so that the total conductivity might show some peculiarities specific both for the quantum and classical transport.

In the first part of the paper we calculate MR and the Hall coefficient of graphene with the short-range disorder assuming that $\max(T,\mu) \gg \hbar\Omega$ and, consequently, the number of filled LLs is large.

The most interesting finding is related to the case $\varepsilon_* \to 0$ ($H \to 0$). We demonstrate that the dominant contribution to the low-field resistivity comes from the energy scale ε_*, which is deep below $\max(T,\mu)$ in this case. This contribution is calculated within SCBA based on the approach of Ref. [7]. Assuming that temperature is not too small,

$$\hbar\omega_c(\varepsilon^*) \ll T \qquad (12)$$

(this condition ensures that the Shubnikov–de Haas oscillations are suppressed by energy averaging within the temperature window) we find that for low fields ($\varepsilon_* \ll T$) the relative longitudinal resistivity scales as a square root of H:

$$\frac{\Delta\varrho_{xx}}{\varrho_{xx}(0)} \approx \frac{0.784\varepsilon_*}{T\cosh^2(\mu/2T)} \propto \sqrt{H}. \qquad (13)$$

Here $\Delta\varrho_{xx} = \varrho_{xx}(H) - \varrho_{xx}(0)$, and $\varrho_{xx}(0) = 1/\sigma_0$. For $T \ll \mu$, MR is exponentially small because the energy scale $\varepsilon \sim \varepsilon^*$ is well beyond the temperature window. However, for $T \gtrsim \mu$, low-field MR is quite large and increases with decreasing the temperature. From the side of the lowest fields, the square-root dependence (13) is limited by exponentially small fields corresponding to $\varepsilon_* \sim \varepsilon_*^{\min} \approx \Delta e^{-\pi\gamma/2}$. Calculation of MR at $\varepsilon_* \ll \varepsilon_*^{\min}$ is not controlled because at such energies γ is renormalized to unity,[17] so that impurity potential becomes effectively strong and SCBA fails. One may expect that for $\varepsilon_* \ll \varepsilon_*^{\min}$ MR becomes parabolic which implies that one should replace factor ε_*/T with $(\varepsilon_*/T)(\varepsilon_*/\varepsilon_*^{\min})^3$ in Eq. (13).

We show that the square-root dependence of MR is also obtained in the opposite limit of large field, $\varepsilon_* \to \infty$ ($H \to \infty$):

$$\frac{\Delta\varrho_{xx}}{\varrho_{xx}(0)} \approx \begin{cases} 0.96\varepsilon_* T/\mu^2, & \text{for} \quad T \gg \mu, \quad \text{and} \quad \varepsilon_* \gg T^2/\mu, \\ 0.68\varepsilon_*/\mu, & \text{for} \quad \mu \gg T, \quad \text{and} \quad \varepsilon_* \gg \mu. \end{cases} \qquad (14)$$

Furthermore, we discuss the behavior of the Hall coefficient R as a function of the magnetic field and the electron concentration and demonstrate that it is a nonmonotonic function of both variables.

In Fig. 1 we plotted schematically the dependence of the longitudinal resistivity and the Hall coefficient on the magnetic
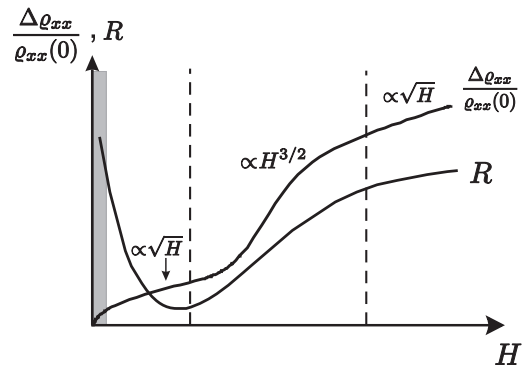

FIG. 1. Schematic plot of the dependence of the longitudinal resistivity and the Hall coefficient on the magnetic field for $\mu \ll T$. Region of exponentially weak fields corresponding to $\varepsilon_* < \varepsilon_{\min}$ is marked by the gray color. Our theory is applicable for higher fields. Vertical dashed lines correspond to $\varepsilon_* \sim T$ and $\varepsilon_* \sim T^2/\mu$.

field for $\mu \ll T$. Importantly, square-root MR is predicted both for very low and very high fields. More detailed pictures are presented below (see Figs. 4–6). It is more convenient to plot all dependencies not as functions of H but as function of $\varepsilon_* \propto \sqrt{H}$. This allows us to present the results for $\mu \ll T$ and $\mu \gg T$ in a similar way.

In the second part of the paper, we analyze the case of the charged impurities and discuss the effect of the electron-electron interaction on magnetotransport. The role of the interaction turns out to be twofold: Interaction leads to a screening of the charged impurities and provides an additional scattering channel which limits conductivity of graphene at the Dirac point (in contrast to a conventional semiconductor). The importance of both effects depends on the value of the dimensionless parameter α which characterizes the strength of the Coulomb interaction. In this work, we use α as a parameter of the theory. Specifically, in the case of charged impurities we discuss separately two cases: $\alpha \sim 1$ and $\alpha \ll 1$. We first neglect electron-electron collisions and demonstrate that for weak coupling ($\alpha \ll 1$) charged impurities yield square-root (parabolic) MR at the Dirac point in the low- (high-)field limit. Then we present a qualitative discussion of the role of inelastic collisions and establish conditions of the applicability of our results in the context of the hydrodynamic treatment. Specifically, we compare our results with those obtained in the collision-dominated regime in Ref. 13 and discuss competition between the two mechanisms of the strong MR at the Dirac point: (i) due to inelastic collisions[13] and (ii) due to screened charged impurities. In particular, we show that the external screening of the charged impurities by the gate electrode favors the disorder-dominated mechanism, so that the square-root low-field MR is always established in a generic gated (i.e., typical for most transport experiments) setup at sufficiently low temperatures. The competition of the electron-electron collisions and scattering of the short-range impurities is also discussed and the conditions needed for realization of the square-root MR are presented.

II. BASIC EQUATIONS

A. Qualitative analysis

In the beginning of this section, before turning to the rigorous calculations, it is instructive to make some qualitative estimates clarifying the physics of the predicted square-root MR. To this end we note that behavior similar to that given by Eq. (13) may be obtained already within the semiclassical Drude-Boltzmann approximation. The main ingredient needed for obtaining the square-root MR is the specific energy dependence of ω_c and τ_{tr} given by Eqs. (3) and (7), respectively. Indeed, the classical approach based on the Boltzmann kinetic equation yields

$$\sigma_{xx}^D(\varepsilon) = \frac{\sigma_0}{1 + [\omega_c(\varepsilon)\tau_{tr}(\varepsilon)]^2} \tag{15}$$

$$= \sigma_0 \left(1 - \frac{4\varepsilon_*^4}{\varepsilon^4 + 4\varepsilon_*^4} \right), \tag{16}$$

where we used Eqs. (7)–(9). Importantly, the second term in the right-hand side of Eq. (16) is peaked near $\varepsilon = 0$ within the width on the order of ε_*. Let us consider for simplicity the case

$\mu \ll T$ assuming that $\varepsilon_* \ll T$. Averaging of Eq. (16) over energy within the temperature window yields two terms: the field-independent contribution σ_0 and the contribution of the peak,

$$\Delta\sigma_{xx}(H) \sim -(\varepsilon_*/T)\sigma_0. \tag{17}$$

Analogously, for the transverse conductivity we obtain

$$\sigma_{xy}^D(\varepsilon) = \omega_c \tau_{tr} \sigma_{xx}^D = \sigma_0 \frac{\varepsilon|\varepsilon|\varepsilon_*^2}{\varepsilon^4 + 4\varepsilon_*^4}. \tag{18}$$

After averaging over energy, Eq. (18) yields

$$\sigma_{xy}^D \sim \sigma_0 \frac{\varepsilon_*\mu}{T^2} \sim \frac{\mu}{T} |\Delta\sigma_{xx}(H)|, \tag{19}$$

so that the total transverse conductivity is smaller[18] than the field-dependent part, $\Delta\sigma_{xx}(H)$, of the longitudinal conductivity. The longitudinal resistivity reads

$$\varrho_{xx}(H) = \frac{\sigma_0 + \Delta\sigma_{xx}(H)}{[\sigma_0 + \Delta\sigma_{xx}(H)]^2 + \left[\sigma_{xy}^D(H)\right]^2}$$

$$\approx \frac{1}{\sigma_0} - \frac{\sigma_0 \Delta\sigma_{xx}(H) + \left[\sigma_{xy}^D(H)\right]^2}{\sigma_0^3}. \tag{20}$$

Since in our case,

$$\left[\sigma_{xy}^D(H)\right]^2 \ll \sigma_0 |\Delta\sigma_{xx}(H)|, \tag{21}$$

we can neglect σ_{xy}^D in Eq. (20). As a result, in contrast to the conventional case of a parabolic spectrum [where $\sigma_{xy}^2 = -\sigma_0 \Delta\sigma_{xx}(H)$], the magnetic-field dependence of $\sigma_{xx}(H)$ directly translates into the MR:

$$\varrho_{xx}(H) \simeq \frac{1}{\sigma_{xx}^D(H)}. \tag{22}$$

Hence, we find

$$\frac{\Delta\varrho_{xx}}{\varrho_{xx}(0)} \simeq -\frac{\Delta\sigma_{xx}(H)}{\sigma_0} \sim \frac{\varepsilon_*}{T} \propto \sqrt{H}. \tag{23}$$

It turns out, however, that this analysis yields an incorrect value of the numerical coefficient in the low-field asymptotic of MR [see discussion after Eq. (60)]. Indeed, a purely classical Drude-Boltzmann approach is valid for $\varepsilon \gg \varepsilon_*$ and fails at relevant energies $\varepsilon \sim \varepsilon_*$ where the LLs start to separate. For $\varepsilon \ll \varepsilon_*$, the LLs are well separated and the longitudinal conductivity contains the density of states squared. After thermal averaging this also leads to a $\sqrt{H}$ contribution to MR which comes from the separated LLs (see, e.g., Refs. 19 and 22) and has essentially quantum nature (despite that the temperature is higher than the interlevel distance). In the calculations below we use a rigorous approach based on the SCBA, which treats both, classical and quantum, mechanisms of the square-root MR on equal footing and allows one to describe crossover between the classical and quantum regions at $\varepsilon \sim \varepsilon_*$.

B. Self-consistent Born approximation for graphene with short-range disorder

Inequality (5) ensures that disorder does not mix two equivalent valleys of graphene, so that one may calculate the conductivity in one valley and then simply multiply the

obtained result by the factor 2. The single-valley Hamiltonian in the perpendicular magnetic field is given by[15,16]

$$\hat{H} = \hat{H}_0 + \hat{V}(\mathbf{r}),$$
$$\hat{H}_0 = v\hbar\left(\hat{\boldsymbol{\sigma}} \cdot \left[\hat{\mathbf{k}} + \frac{e}{c\hbar}\mathbf{A}(\mathbf{r})\right]\right),$$

where e is the absolute value of the electron charge, and $\hat{V}(\mathbf{r})$ is given by Eq. (6). The eigenenergies and eigenfunctions of H_0 read

$$\varepsilon_n = \hbar\Omega\,\text{sign}(n)\sqrt{2|n|}, \quad \psi_{n,k}(x,y) = e^{-iky}\chi_n\big(x - kl_H^2\big), \quad (24)$$

where Ω is given by Eq. (4) and

$$\chi_n(x) = \begin{cases} \frac{1}{\sqrt{2}}\begin{bmatrix} h_{|n|-1}(x) \\ \text{sign}(n)h_{|n|}(x) \end{bmatrix}, & \text{for} \quad n = \pm 1, \pm 2, \dots; \\ \begin{bmatrix} 0 \\ h_0(x) \end{bmatrix}, & \text{for} \quad n = 0. \end{cases} \quad (25)$$

Here $h_n(x)$ are the normalized wave functions of the harmonic oscillator with the frequency Ω and mass $\hbar/vl_H$. As seen from Eq. (24), the energy-dependent cyclotron frequency is connected with Ω by Eq. (3) while the relevant energy scale ε_* is given by Eq. (10) and corresponds to high LLs, so that we can use the SCBA for calculation of the resistivity.

In the SCBA, the electron Green function in the short-range potential is given by[7]

$$\hat{G}(\varepsilon) = \frac{1}{\varepsilon - \hat{H}_0 - \hat{\Sigma}}, \quad (26)$$

where self-energy is found from the following equation:

$$\hat{\Sigma} = \kappa\left\langle\mathbf{r}\left|\frac{1}{\varepsilon - \hat{H}_0 - \hat{\Sigma}}\right|\mathbf{r}\right\rangle. \quad (27)$$

As shown in Ref. 7, $\hat{\Sigma}$ is 2×2 matrix having nonzero matrix elements between χ_n and χ_{-n}. However, at high energies corresponding to high Landau levels, $\hat{\Sigma}$ becomes simply proportional to the unit matrix:

$$\hat{\Sigma}(\varepsilon) \approx \Sigma(\varepsilon)\begin{pmatrix} 1 & 0 \\ 0 & 1 \end{pmatrix}, \quad \text{for} \quad \varepsilon \gg \hbar\Omega,$$

where

$$\Sigma(\varepsilon) = \Delta(\varepsilon) \pm i\Gamma(\varepsilon) \quad (28)$$

(signs $+$ and $-$ corresponds to advanced and retarded self-energies, respectively). In this approximation, Σ obeys[7]

$$\Sigma = \frac{(\hbar\Omega)^2}{\gamma}\sum_{n=0}^{N_{\max}}\frac{\varepsilon - \Sigma}{(\varepsilon - \Sigma)^2 - \varepsilon_n^2}. \quad (29)$$

Here $N_{\max}$ is the ultraviolet cutoff. The sum entering Eq. (29) can be calculated by using the identity,

$$\sum_{n=0}^{N_{\max}}\frac{1}{N - W} \approx \ln\left(\frac{N_{\max}}{W}\right) - \pi\cot(\pi W), \quad (30)$$

valid for $N_{\max} \gg \text{Re}(W) \gg 1$, $\text{Im}(W) \lesssim \text{Re}(W)$, and $\text{Im}(W) > 0$. From Eqs. (29) and (30) we obtain

$$\Sigma \approx \frac{\varepsilon - \Sigma}{2\gamma}\left\{\ln\left[\frac{2N_{\max}(\hbar\Omega)^2}{(\varepsilon - \Sigma)^2}\right] - \pi\cot\left[\pi\frac{(\varepsilon - \Sigma)^2}{2(\hbar\Omega)^2}\right]\right\}. \quad (31)$$

The logarithm entering Eq. (31) is a smooth function of ε and leads to a linear in ε correction to Σ, which is irrelevant provided that $\gamma \gg \ln N_{\max}$ (see also discussion of SCBA in graphene in Ref. 12). We substract this correction from Σ and for simplicity use the same notation Σ for thus redefined self-energy. Then we find from Eq. (31) the system of coupled equations for Δ and Γ:

$$\Delta = \frac{\Gamma_0\sin\left[2\pi(\varepsilon - \Delta)/\hbar\omega_c\right]}{\cosh\left[2\pi\Gamma/\hbar\omega_c\right] - \cos\left[2\pi(\varepsilon - \Delta)/\hbar\omega_c\right]}, \quad (32)$$

$$\Gamma = \frac{\Gamma_0\sinh\left[2\pi\Gamma/\hbar\omega_c\right]}{\cosh\left[2\pi\Gamma/\hbar\omega_c\right] - \cos\left[2\pi(\varepsilon - \Delta)/\hbar\omega_c\right]}, \quad (33)$$

where $\Gamma_0(\varepsilon) = \hbar/2\tau_q(\varepsilon)$. We also normalize Γ by its value at zero magnetic field introducing the quantity,

$$z(\varepsilon) = \frac{\Gamma(\varepsilon)}{\Gamma_0(\varepsilon)} = \frac{\nu(\varepsilon)}{\nu_0(\varepsilon)}. \quad (34)$$

Here $\nu(\varepsilon)$ is the density of states in the magnetic field. The solution of Eqs. (32) and (33) can be found analytically in the limiting cases $\varepsilon \gg \varepsilon_*(x \ll 1)$ and $\varepsilon \ll \varepsilon_*(x \gg 1)$:

$$\Delta = \begin{cases} 2\Gamma_0 e^{-\pi/x}\sin\left(\frac{2\pi\varepsilon}{\hbar\omega_c}\right), & \text{for} \quad \varepsilon \gg \varepsilon_*; \\ \sum_n \vartheta\left(\frac{\varepsilon - \varepsilon_n}{\Gamma_n}\right)\frac{\varepsilon}{2}, & \text{for} \quad \varepsilon \ll \varepsilon_*, \end{cases} \quad (35)$$

$$z \approx \begin{cases} 1 + 2ae^{-\pi/x} + 2(2a^2 - 1)\left(1 - \frac{2\pi}{x}\right)e^{-2\pi/x}, & \text{for} \quad \varepsilon \gg \varepsilon_*; \\ \sqrt{\frac{2x}{\pi}}\sum_n \vartheta\left(\frac{\varepsilon - \varepsilon_n}{\Gamma_n}\right)\sqrt{1 - \left(\frac{\varepsilon - \varepsilon_n}{\Gamma_n}\right)^2}, & \text{for} \quad \varepsilon \ll \varepsilon_*. \end{cases} \quad (36)$$

Here

$$a = \cos\left(\frac{2\pi\varepsilon}{\hbar\omega_c}\right), \quad (37)$$

$\vartheta(y)$ is equal to unity (zero) for $|y| < 1$ ($|y| > 1$) and

$$\Gamma_n = \Gamma(\varepsilon_n) = \hbar\sqrt{\frac{2\omega_c(\varepsilon_n)}{\pi\tau_q(\varepsilon_n)}}. \quad (38)$$

In the first line of Eq. (36) we expanded z up to the second order with respect to $\exp(-\pi/x)$. As seen from Eqs. (3), (7), and (38), Γ_n actually does not depend on n for the case of short-range disorder which we concern with: $\Gamma_n = \Gamma_\Omega =$ const. Here

$$\Gamma_\Omega = \hbar\Omega\sqrt{\frac{2}{\pi\gamma}}. \quad (39)$$
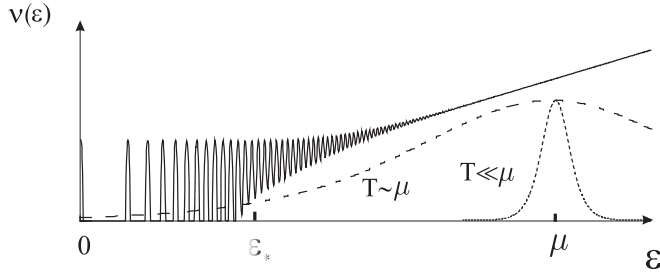
FIG. 2. Density of the electron states in graphene with short-range disorder (solid line) and the derivative of the Fermi function, $-\partial n_F/\partial \varepsilon$, for the temperatures $T \ll \mu$ and $T \sim \mu$ (dashed lines).

Hence, the widths of different LLs are equal, but the distance $\hbar\omega_c$ between neighbor LLs decreases with increasing ε. We also see that self-energy changes periodically with ε on the scale $\hbar\omega_c$. Both the period and the shape of these oscillations slowly depend on the energy due to energy dependence of x. The density of electron states, $\nu(\varepsilon)$, following from Eqs. (34) and (36) is plotted in Fig. 2 for $\varepsilon_* \ll \mu$. At low energies, $x \ll 1$, LLs are well separated, while for $x \gg 1$ density of states is given by zero-field density, Eq. (2), up to exponentially small oscillating terms.

III. CALCULATION OF THE CONDUCTIVITY

The conductivity tensor is given by thermal averaging of the energy-dependent tensor $\sigma_{ij}(\varepsilon)$:

$$\sigma_{ij} = \int_{-\infty}^{\infty} d\varepsilon \left[-\frac{\partial n_F(\varepsilon)}{\partial \varepsilon} \right] \sigma_{ij}(\varepsilon), \tag{40}$$

where $n_F(\varepsilon)$ is the Fermi distribution function.

The longitudinal conductivity $\sigma_{xx}(\varepsilon)$ is calculated by summation of the ladder diagrams.[7] The result is given by Eq. (4.13) of Ref. 7. Using Eq. (30) one may rewrite this result in terms of $z(\varepsilon)$:

$$\sigma_{xx}(\varepsilon) = \sigma_0 \frac{z(\varepsilon)^2}{z(\varepsilon)^2 + [\omega_c(\varepsilon)\tau_{\text{tr}}(\varepsilon)]^2}. \tag{41}$$

For high energies $x \to 0$, so that $z \to 1$ [see Eq. (36)] and we obtain Drude result, Eq. (15).

For $x \gg 1$, we find from Eqs. (41) and (36) the conductivity near nth LL,[7]

$$\sigma_{xx}(\varepsilon) = \begin{cases} \frac{2e^2 n}{\pi^2 \hbar} \left[1 - \left(\frac{\varepsilon - \varepsilon_n}{\Gamma_\Omega} \right)^2 \right], & \text{for} \quad |\varepsilon - \varepsilon_n| < \Gamma_\Omega, \\ 0, & \text{for} \quad |\varepsilon - \varepsilon_n| > \Gamma_\Omega. \end{cases} \tag{42}$$

We note that Eq. (41) may be obtained from Eq. (15) by replacement of $1/\tau_{\text{tr}}(\varepsilon)$ with $z(\varepsilon)/\tau_{\text{tr}}(\varepsilon)$. Hence, the only difference of the SCBA result, compared to the Drude one is the renormalization of the density of states given by Eq. (34).

The calculation of $\sigma_{xy}(\varepsilon)$ is more subtle. Simplest approximation based on summation of the ladder diagrams leads to Drude-like formula with renormalized scattering rate,

$$\sigma_{xy}^I(\varepsilon) = \sigma_0 \frac{\omega_c(\varepsilon)\tau_{\text{tr}}(\varepsilon)z(\varepsilon)}{z^2(\varepsilon) + [\omega_c(\varepsilon)\tau_{\text{tr}}(\varepsilon)]^2}, \tag{43}$$

in a full analogy with Eq. (41). In fact, there also exists another contribution to the transverse conductivity, which is expressed

via thermodynamical properties of the electron gas:[20,21]

$$\sigma_{xy}^{II}(\varepsilon) = ec[\partial n/\partial H]_\varepsilon. \tag{44}$$

Here $n = n(\varepsilon, H)$ is the electron concentration in magnetic field for zero temperature and chemical potential coinciding with ε. The derivative over H is taken for fixed ε. Hence,

$$\sigma_{xy}(\varepsilon) = \sigma_{xy}^I(\varepsilon) + \sigma_{xy}^{II}(\varepsilon). \tag{45}$$

In fact, $\sigma_{xy}^{II}(\varepsilon)$ yields essential contribution to $\sigma_{xy}(\varepsilon)$ for $\varepsilon \ll \varepsilon_*$ when LLs are well separated [in the opposite case of overlapping LLs $\sigma_{xy}^{II}(\varepsilon)$ is exponentially small].

Let us now do the integral in Eq. (40). As follows from Eq. (36), the dependence $\sigma_{ij}(\varepsilon)$ contains fast oscillations on the scale $\hbar\omega_c$, the shape and the period of the oscillations being energy dependent due to energy dependence of x. Therefore, for relatively high temperature the integration in Eq. (40) may be performed in two steps. First, we average $\sigma_{ij}(\varepsilon)$ in Eq. (40) by the energy interval $\delta\varepsilon$, such that $\varepsilon \gg \delta\varepsilon \gg \hbar\omega_c(\varepsilon)$. Such an averaging "filters" the Shubnikov-de Haas oscillations and results in a smooth function $\bar{\sigma}_{ij}(\varepsilon)$. One can also show that after averaging $\bar{\sigma}_{xy}^{II}$ can be neglected[23] (provided that $\gamma \gg 1$) both for overlapping[24] ($\varepsilon \gg \varepsilon_*$) and for separated ($\varepsilon \ll \varepsilon_*$) LLs. Hence below we use

$$\bar{\sigma}_{xy}(\varepsilon) \approx \bar{\sigma}_{xy}^I(\varepsilon).$$

It is convenient to write $\bar{\sigma}_{ij}$ in the following form:

$$\bar{\sigma}_{ij}(\varepsilon) = \sigma_{ij}^D(\varepsilon) \eta_{ij}(\varepsilon), \tag{46}$$

where $\eta_{ij}(\varepsilon)$ are dimensionless factors. From Eqs. (36), (37), (41), and (43) we find asymptotical behavior of η_{ij}:

$$\eta_{xx} \approx \begin{cases} 1 - 24x^2 e^{-2\pi/x} = 1 - \frac{24\varepsilon_*^4}{\varepsilon^4} e^{-2\pi\varepsilon^2/\varepsilon_*^2}, & \text{for} \quad \varepsilon \gg \varepsilon_*, \\ C_1\sqrt{x} = C_1\varepsilon_*/\varepsilon, & \text{for} \quad \varepsilon \ll \varepsilon_*, \end{cases} \tag{47}$$

$$\eta_{xy} \approx \begin{cases} 1 + 2e^{-2\pi/x} = 1 + 2e^{-2\pi\varepsilon^2/\varepsilon_*^2}, & \text{for} \quad \varepsilon \gg \varepsilon_*, \\ 1, & \text{for} \quad \varepsilon \ll \varepsilon_*. \end{cases} \tag{48}$$

Here $C_1 = 8\sqrt{2}/3\pi\sqrt{\pi} \approx 0.68$. For arbitrary values of ε the factors η_{ij} have been calculated numerically. The dependencies $\bar{\sigma}_{xx}(\varepsilon)$ and $\bar{\sigma}_{xy}(\varepsilon)$ are plotted schematically in Fig. 3. In this picture we took into account that $\sigma_{xx}(\varepsilon) = \sigma_{xx}(-\varepsilon)$, $\sigma_{xy}(\varepsilon) = -\sigma_{xy}(-\varepsilon)$ because of the particle-hole symmetry. In the high-energy asymptotics we keep exponentially small terms [proportional to $\exp(-2\pi/x)$], since they are important in the calculation of MR in the limit of low temperature and low field (see below). It is worth also noting that averaged longitudinal conductivity is not exactly zero at $\varepsilon = 0$ but saturates at $\varepsilon \sim \hbar\Omega$ at a quite small value: $\bar{\sigma}_{xx} \sim \sigma_0/\gamma^{3/2} \ll \sigma_0$.

As a second step, we calculate σ_{ij} by replacing $\sigma_{ij}(\varepsilon)$ with $\bar{\sigma}_{ij}(\varepsilon)$ in Eq. (40):

$$\sigma_{ij} = \int_{-\infty}^{\infty} d\varepsilon \left[-\frac{\partial n_F(\varepsilon)}{\partial \varepsilon} \right] \bar{\sigma}_{ij}(\varepsilon), \tag{49}$$

and substitute thus obtained σ_{ij} into expression for the longitudinal resistivity:

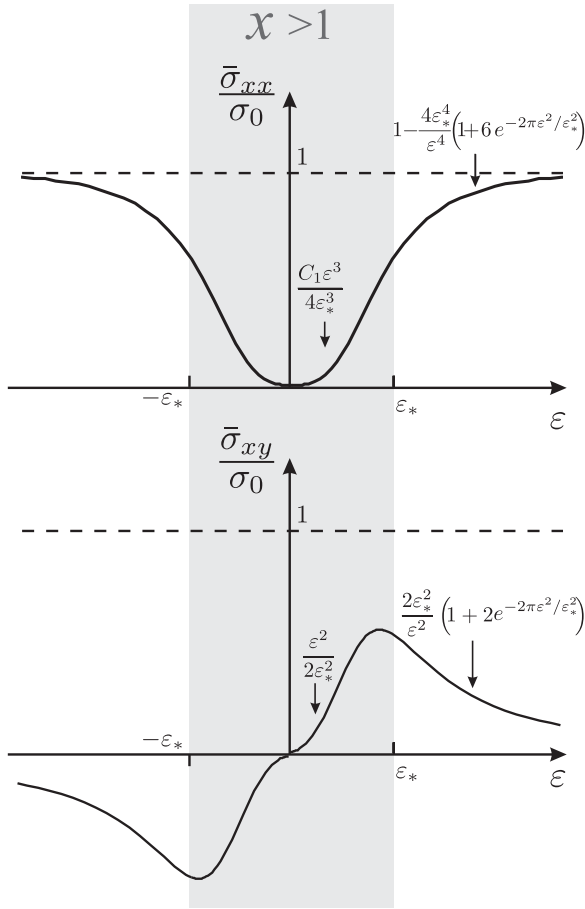$$\varrho_{xx} = \frac{\sigma_{xx}}{\sigma_{xx}^2 + \sigma_{xy}^2}. \tag{50}$$

FIG. 3. Dependence of $\bar{\sigma}_{xx}$ and $\bar{\sigma}_{xy}$ on energy. The region $x > 1$ is marked by gray color.

The result of calculations depends on the relation between three relevant energies T, μ, and ε_*. The magnetic field dependence of ϱ_{xx} is encoded in the square-root scaling of ε_*. Below we discuss separately the cases of low and high temperatures.

A. Low temperatures $T \ll \mu$.

We start with discussing of the high-field limit $\varepsilon_* \gg \mu$. Since integral over energy in Eq. (49) is concentrated in the narrow temperature window near $\varepsilon = \mu$ we can use low energy asymptotics for $\bar{\sigma}_{xx}$ and $\bar{\sigma}_{xy}$; see Fig. 3. Doing so, and replacing in Eq. (49) $[-\partial n_F(\varepsilon)/\partial \varepsilon]$ with $\delta(\varepsilon - \mu)$, we find

$$\sigma_{xx} \approx \sigma_0 \frac{C_1 \mu^3}{4\varepsilon_*^3}, \quad \sigma_{xy} \approx \sigma_0 \frac{\mu^2}{2\varepsilon_*^2}. \tag{51}$$

We see that $\sigma_{xx} \ll \sigma_{xy}$. Therefore, $\varrho_{xx} \approx \sigma_{xx}/\sigma_{xy}^2$ and

$$\frac{\Delta \varrho_{xx}}{\varrho_{xx}(0)} \approx \frac{C_1 \varepsilon_*}{\mu} \propto \sqrt{H}, \quad \text{for} \quad \varepsilon_* \gg \mu. \tag{52}$$

Next we consider the opposite case $\varepsilon_* \ll \mu$. In this case, there are different competing contributions to the MR. First contribution is obtained quite analogously to the high-field limit by replacing the derivative from the Fermi distribution with the delta function. In this approximation, $\sigma_{xx} = \bar{\sigma}_{xx}(\mu)$, $\sigma_{xy} = \bar{\sigma}_{xy}(\mu)$. As follows from Eqs. (47) and (48), in the limit

of large μ these conductivities differ from Drude values by exponentially small terms only. It is well known that in the Drude-Boltzmann approximation MR is absent in the limit of low T. Hence, MR should be exponentially small. Indeed, substituting $\bar{\sigma}_{xx}(\mu)$ and $\bar{\sigma}_{xy}(\mu)$ into Eq. (50), using Eqs. (46), (47), and (48), and keeping terms on the order of $\exp(-2\pi/x)$ we obtain

$$\frac{\Delta \varrho_{xx}}{\varrho_{xx}(0)} \approx \frac{8\varepsilon_*^4}{\mu^4} e^{-2\pi\mu^2/\varepsilon_*^2}, \quad \text{for} \quad \varepsilon_* \ll \mu. \tag{53}$$

There are two other contributions which may compete with this exponentially small result. Both contributions arise due to the finite value of temperature, which was in fact assumed to be zero while deriving Eq. (53). Let us now take into account that the function,

$$-\frac{\partial n_F(\varepsilon)}{\partial \varepsilon} = \frac{1}{4T \cosh^2[(\varepsilon - \mu)/2T]}, \tag{54}$$

is peaked near $\varepsilon = \mu$ within a finite width on the order of T. First of all, there exists a correction to the MR due to a small variation of $x(\varepsilon)$ within the temperature window. To find this correction we put $\eta_{ij} \approx 1$, expand $\bar{\sigma}_{ij}(\varepsilon)$ near $\varepsilon = \mu$ up to the second order with respect to $\varepsilon - \mu$, calculate integral Eq. (49) and use Eq. (50). As a result, we get a quadratic-in-H MR,

$$\frac{\Delta \varrho_{xx}}{\varrho_{xx}(0)} = \frac{C_2 T^2 \varepsilon_*^4}{\mu^6} \propto H^2, \tag{55}$$

where $C_2 \approx 16\pi^2/3$. This correction becomes larger than Eq. (53) for relatively weak fields such that $\varepsilon_* \ll \varepsilon_1$, where

$$\varepsilon_1 = \frac{\sqrt{2\pi}\,\mu}{\ln^{1/2}(8\mu^2/C_2 T^2)}. \tag{56}$$

At very low magnetic fields, another contribution comes into play, namely, the contribution to integral Eq. (49) from the energies $\varepsilon \sim \varepsilon^*$ which are well beyond the temperature window. To find this contribution we first write $\bar{\sigma}_{xx}(\varepsilon)$ in the following way:

$$\bar{\sigma}_{xx}(\varepsilon) = \sigma_0[1 - f(\varepsilon/\varepsilon_*)]. \tag{57}$$

The function $f(y)$ has maximum at $y = 0$ and decays when y becomes larger than 1, or, equivalently, ε becomes larger than ε_* (see Fig. 3):

$$f(y) \approx \begin{cases} \frac{4}{y^4}, & \text{for} \quad y \gg 1 (\varepsilon \gg \varepsilon_*); \\ 1 - C_1 y^3/4, & \text{for} \quad y \ll 1 (\varepsilon \ll \varepsilon_*). \end{cases} \tag{58}$$

Here we neglected exponentially small corrections to f at large ε and introduced dimensionless variable $y = \varepsilon/\varepsilon_* = 1/\sqrt{x}$. Let us now assume that ε^* is smaller than T. Then one can replace $[-\partial n_F(\varepsilon)/\partial \varepsilon]$ with its value at zero energy $-n_F'(0)$, while calculating the contribution to σ_{xx} coming from the region $\varepsilon \sim \varepsilon^*$. Doing so, we obtain

$$\sigma_{xx} = \sigma_0[1 - 2C_3 \varepsilon_* |n_F'(0)|], \tag{59}$$

where dimensionless constant C_3 is given by the integral,

$$C_3 = \int_0^\infty dy\, f(y) = 1.568. \tag{60}$$

It is instructive to compare the obtained result with the "purely classical" calculation which ignores the existence of LLs. On

the formal level, such an approximation implies replacement η_{ij} with unity in Eq. (46). Simple calculation (see also discussion in Sec. II A) shows that thus calculated conductivity can be presented in the same form as Eq. (59), where one should replace C_3 with

$$
\begin{aligned}
C_3^D &= \int_0^\infty dy \left(1 - \frac{1}{1 + 4x^2} \right) \\
&= \int_0^\infty dy \frac{4}{y^4 + 4} = \pi/2 = 1.571.
\end{aligned} \tag{61}
$$

This value is close but different from C_3, so that discreteness of LLs should be taken into account.

Now we are ready to calculate resistivity correction. In the regime under discussion ($\varepsilon_* \ll T \ll \mu$), $\sigma_{xx} \gg \sigma_{xy}$, so that $\varrho_{xx} \approx 1/\sigma_{xx}$ and

$$
\frac{\Delta \varrho_{xx}}{\varrho_{xx}(0)} \approx 2 C_3 \varepsilon_* |n_F'(0)| \propto \sqrt{H}. \tag{62}
$$

Since $T \ll \mu$, we conclude that MR is exponentially small:

$$
\frac{\Delta \varrho_{xx}}{\varrho_{xx}(0)} \approx \frac{2 C_3 \varepsilon_*}{T} e^{-\mu/T}. \tag{63}
$$

Comparing Eq. (63) with Eq. (55), we see that the former contribution dominates when $\varepsilon_* \ll \varepsilon_2$, where

$$
\varepsilon_2 \sim \frac{\mu^2}{T} e^{-\mu/3T} \ll T. \tag{64}
$$

Therefore, in accordance with our assumption, $\varepsilon_* \ll T$ in the regime when Eq. (63) dominates.

Looking now more attentively at the above derivation one concludes that Eq. (62) is valid at the arbitrary relation between T and μ provided that $\varepsilon_* \to 0$ (but $\varepsilon_* > \varepsilon_*^{\min}$). Hence, the low-field MR is given by

$$
\frac{\Delta \varrho_{xx}}{\varrho_{xx}(0)} \approx \frac{C_3 \varepsilon_*}{2T \cosh^2(\mu/2T)} \propto \sqrt{H}. \tag{65}
$$

B. High temperatures $\mu \ll T$.

In this case, the low field asymptotics of MR is realized at $\varepsilon_* \ll T$ and is given by Eq. (65), where one can put $\mu = 0$,

$$
\frac{\Delta \varrho_{xx}}{\varrho_{xx}(0)} \approx \frac{C_3 \varepsilon_*}{2T} \propto \sqrt{H}/T, \quad \text{for} \quad \varepsilon_* \ll T. \tag{66}
$$

Hence, near the Dirac point resistivity correction scales as $\sqrt{H}$ at $H \to 0$, and increases (for fixed H) with decreasing the temperature.

Let us now consider larger fields, $\varepsilon_* \gg T$. In this case, one can use low-energy asymptotics,

$$
\bar{\sigma}_{xx}(\varepsilon) \approx \frac{C_1}{4} \frac{|\varepsilon|^3}{\varepsilon_*^3}, \quad \bar{\sigma}_{xy}(\varepsilon) \approx \frac{\sigma_0}{2} \frac{\varepsilon |\varepsilon|}{\varepsilon_*^2}. \tag{67}
$$

Thermal averaging yields

$$
\begin{aligned}
\sigma_{xx} &= \frac{\sigma_0 C_1}{16} \int_0^\infty d\varepsilon \frac{\varepsilon^3}{\varepsilon_*^3 T} \left[\frac{1}{\cosh^2 \left(\frac{\varepsilon - \mu}{2T} \right)} + \frac{1}{\cosh^2 \left(\frac{\varepsilon + \mu}{2T} \right)} \right] \\
&\approx \frac{9 \sigma_0 C_1 \zeta(3)}{4} \frac{T^3}{\varepsilon_*^3},
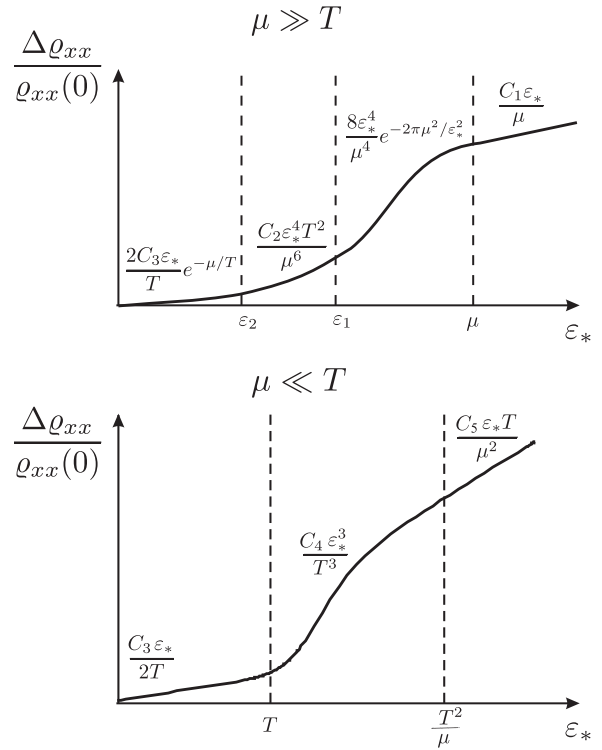\end{aligned} \tag{68}
$$

FIG. 4. Resistivity of graphene for the cases $T \ll \mu$ and $T \gg \mu$ as a function of $\varepsilon_* \propto \sqrt{H}$.

$$
\begin{aligned}
\sigma_{xy} &= \frac{\sigma_0}{8} \int_0^\infty d\varepsilon \frac{\varepsilon^2}{\varepsilon_*^2 T} \left[\frac{1}{\cosh^2 \left(\frac{\varepsilon - \mu}{2T} \right)} - \frac{1}{\cosh^2 \left(\frac{\varepsilon + \mu}{2T} \right)} \right] \\
&\approx 2 \sigma_0 \ln 2 \frac{\mu T}{\varepsilon_*^2},
\end{aligned} \tag{69}
$$

where ζ is Riemann zeta function, $\zeta(3) \approx 1.2$. From Eqs. (68) and (69) we find

$$
\begin{aligned}
\frac{\Delta \varrho_{xx}}{\varrho_{xx}(0)} &\approx \frac{4}{9 C_1 \zeta(3)} \frac{\varepsilon_*^3}{T^3} \frac{1}{1 + \left[\frac{8 \ln 2}{9 C_1 \zeta(3)} \right]^2 \frac{\mu^2 \varepsilon_*^2}{T^4}} \\
&\approx \begin{cases} C_4 \varepsilon_*^3/T^3, & \text{for} \quad T \ll \varepsilon_* \ll T^2/\mu; \\ C_5 \varepsilon_* T/\mu^2, & \text{for} \quad T^2/\mu \ll \varepsilon_*. \end{cases}
\end{aligned} \tag{70}
$$

Here $C_4 = 4/9 C_1 \zeta(3) \approx 0.54$, $C_5 = 9 C_1 \zeta(3)/16(\ln 2)^2 \approx 0.96$.

The results of calculations are summarized in Fig. 4.

IV. HALL COEFFICIENT

Using the equations derived above one can easily calculate the transverse resistivity $\varrho_{xy} = \sigma_{xy}/(\sigma_{xx}^2 + \sigma_{xy}^2)$ and the Hall coefficient,

$$
R = \frac{\varrho_{xy}}{H}. \tag{71}
$$

Below we discuss the dependence of R on H and on the charge density at zero field,

$$
n = \int_{-\infty}^\infty n_F(\varepsilon) v_0(\varepsilon) d\varepsilon - \int_{-\infty}^0 v_0(\varepsilon) d\varepsilon. \tag{72}
$$

The second term in the right-hand side of Eq. (72) is the concentration of background electrons which compensate the positive charge of the donors in the neutrality point. One can easily check that $n = 0$ for $\mu = 0$.

For $T \ll \mu$, simple calculation yields that the Hall coefficient up to small corrections is given by the conventional expression,

$$R = \frac{1}{ecn}, \tag{73}$$

both at very low ($\varepsilon_* \ll \mu$) and at very high ($\varepsilon_* \gg \mu$) magnetic field. For $\varepsilon_* \sim \mu$, Eq. (73) is valid up to a numerical factor on the order of unity ($R \sim 1/ecn$). Concentration entering Eq. (73) is given by

$$n \approx \int_0^\mu \nu_0(\varepsilon') d\varepsilon' = \frac{N\mu|\mu|}{4\pi v^2 \hbar^2}. \tag{74}$$

Consider now the vicinity of the Dirac point, $\mu \ll T$. In this case,

$$n \approx \frac{N\mu T \ln 2}{\pi v^2 \hbar^2}, \tag{75}$$

while the transverse conductivity is given by

$$\sigma_{xy} = \int_0^\infty d\varepsilon \frac{\bar{\sigma}_{xy}(\varepsilon)}{4T} \left[\frac{1}{\cosh^2\left(\frac{\varepsilon-\mu}{2T}\right)} - \frac{1}{\cosh^2\left(\frac{\varepsilon+\mu}{2T}\right)} \right]$$
$$\approx \frac{\mu}{2T^2} \int_0^\infty d\varepsilon \bar{\sigma}_{xy}(\varepsilon) \frac{\sinh\left(\frac{\varepsilon}{2T}\right)}{\cosh^3\left(\frac{\varepsilon}{2T}\right)}. \tag{76}$$

For $\varepsilon_* \ll T$, the main contribution to σ_{xy} comes from the energy interval $\varepsilon_* < \varepsilon < T$, where the integral in Eq. (76) is logarithmically divergent. Therefore, one may use large-ε asymptotic, $\bar{\sigma}_{xy} \approx 2\sigma_0 \varepsilon_*^2/\varepsilon^2$, and calculate the integral in the limits ε_* and T. Doing so we find with the logarithmic precision: $\sigma_{xy} \approx \sigma_0 (\mu \varepsilon_*^2/2T^3) \ln(T/\varepsilon_*)$. The longitudinal conductivity is given by Eq. (59) where one can neglect small correction proportional to ε_*/T, thus writing $\sigma_{xx} \approx \sigma_0$. Using these equations we find

$$R = R_0 \ln\left(\frac{T}{\varepsilon_*}\right), \tag{77}$$

where

$$R_0 = \frac{\pi \mu v^2 \hbar^2}{ecNT^3} \sim \frac{n}{ecn_T^2}, \tag{78}$$

where $n_T \sim NT^2/v^2\hbar^2$ is the electron concentration for $\mu \sim T$. Hence, the Hall coefficient logarithmically increases with decreasing the magnetic field. Above we noticed that our calculations are valid up to the exponentially small fields where $\varepsilon_* \sim \Delta e^{-\pi\gamma/2}$. Therefore, the maximal value of the $\ln(T/\varepsilon_*)$ is limited by $\pi\gamma/2 - \ln(\Delta/T)$.

In the opposite case, $\varepsilon_* \gg T$, the conductivity tensor is given by Eqs. (68) and (69) which yield for the Hall coefficient the following expression:

$$R = R_0 \frac{C_6 \varepsilon_*^2/T^2}{1 + C_7 \mu^2 \varepsilon_*^2/T^4}, \tag{79}$$

where $C_6 = 64 \ln 2/[9C_1\zeta(3)]^2 \approx 0.82$ and $C_7 = [8\ln 2/9C_1\zeta(3)]^2 \approx 0.57$. We see that the Hall coefficient
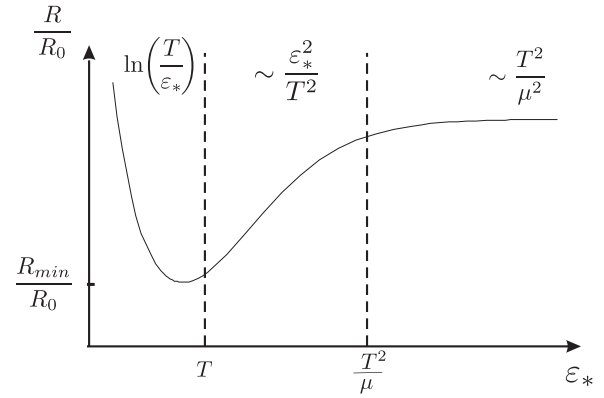

FIG. 5. Dependence of the Hall coefficient, ϱ_{xy}/H, on $\varepsilon_* \propto \sqrt{H}$ at $T \gg \mu$.

linearly increases with the magnetic field, $R \propto \varepsilon_*^2 \propto H$, in the interval $T \ll \varepsilon_* \ll T^2/\mu$ and saturates when ε_* becomes larger than T^2/μ. From Eqs. (78) and (79) we conclude that R is a nonmonotonic function of the magnetic field and has a minimum (for positive μ) at magnetic fields corresponding to $\varepsilon_* \sim T$. The minimal value of R is given by $R_{\min} \sim R_0$. The dependence of R on ε_* is plotted schematically in Fig. 5.

Measurements of the Hall coefficient are usually used for extracting the density of the carriers with the help of conventional expression (73). From Eqs. (75), (77), and (79) we see that such a procedure fails near the Dirac point. Let us, therefore, discuss the dependence of R on n in detail (see also Ref. 26). The analysis of the above equations shows that R is a nonmonotonic function of n both at low and high fields: It turns to zero for $n = 0$, has a maximum at certain $n = n_m$, and decays as $1/n$ according to Eq. (73) for $n \to \infty$ (see Fig. 6).

As follows from Eqs. (75), (77), and (78), at low fields or, equivalently, high temperatures ($\varepsilon_* \ll T$), the Hall coefficient linearly increases with n at $n \ll n_T$ ($\mu \ll T$),

$$R \sim \frac{n}{ecn_T^2} \ln(T/\varepsilon_*), \tag{80}$$

reaches the maximum value,

$$R_{\max} \sim \frac{1}{ecn_T} \ln(T/\varepsilon_*), \tag{81}$$

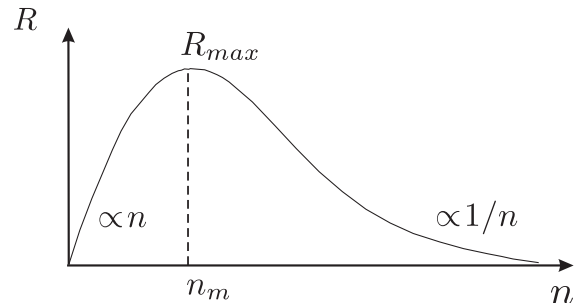at $n_m \sim n_T$ ($\mu \sim T$), and decays inversely proportional to the concentration at $n \to \infty$.[27]

FIG. 6. Dependence of the Hall coefficient on electron concentration.

At high field or low temperatures ($\varepsilon_* \gg T$), the dependence of R on n also has a maximum and is linear at small concentration. However, as seen from Eq. (79) there are some differences compared to the low-field case. First of all, the coefficient in the linear dependence at small n turns out to be different,

$$R \sim \frac{n}{ecn_T^2}\left(\frac{\varepsilon_*}{T}\right)^2. \tag{82}$$

Secondly, the maximum value of R is reached at much smaller concentration $n_m \sim (T/\varepsilon_*)n_T$ corresponding to $\mu \sim T^2/\varepsilon_* \ll T$. Equation (82) holds below this concentration while at larger n the Hall coefficient is given by conventional expression (73). The maximum Hall coefficient reads

$$R_{\max} \sim \frac{1}{ecn_T}\left(\frac{\varepsilon_*}{T}\right). \tag{83}$$

V. CHARGED IMPURITIES

In the previous sections we discussed magnetotransport in graphene with the short-range disorder. One can see from the above derivations that the most interesting result, the square-root MR at low H, is a direct consequence of the energy dependence of scattering time specific for the short-range impurities: $1/\tau_{\rm tr} \propto |\varepsilon|$. In this section we discuss scattering by the charged impurities which are often considered to give a dominant contribution to the resistivity of graphene. In particular, the Coulomb impurities yield a linear dependence of the conductivity on the carrier concentration away from the Dirac point, in agreement with the experimental data on most graphene samples.

The matrix element of the scattering on a single charged impurity is given by

$$V_q = \frac{2\pi e^2/q\varkappa}{1 + (2\pi e^2/q\varkappa)N\Pi(q)}, \tag{84}$$

where $\Pi(q)$ is the static polarization operator and $\varkappa$ is the dielectric constant. If we neglect the screening of the impurities [which corresponds to $\Pi = 0$ in Eq. (84)], and use golden rule for calculation of the transport scattering rate, we get $1/\tau_{\rm tr} \propto |\varepsilon|^{-1}$, which implies that $\omega_c\tau_{\rm tr}$ does not depend on energy and, consequently, the mechanism of the MR discussed above does not work. Note that in contrast to conventional semiconductors, where condition $\omega_c\tau_{\rm tr} = {\rm const}$ guaranties absence of MR, in graphene there should be a parabolic MR (more pronounced for $\mu \lesssim T$) within the model neglecting screening. This is because of a partial cancellation of the electron and hole contributions to the transverse conductivity. In particular, exactly at the Dirac point $\sigma_{xy} = 0$ and hence $\rho_{xx}(H) = 1/\sigma_{xx}(H)$, so that MR is given by $\Delta\varrho_{xx}/\varrho_{xx}(0) = (\omega_c\tau_{\rm tr})^2 \propto H^2$.

Let us now take screening into account. We restrict ourselves to the analysis of the MR at the Dirac point, where one expects the most pronounced effect. The general expression for the polarization operator at the Dirac point was derived in Ref. 25. For our purposes it is sufficient to know the asymptotical expression for $\Pi(q)$ at $q \ll T/\hbar v$:

$$\Pi(q) \approx \frac{T\ln 2}{\pi\hbar^2 v^2}, \quad \text{for} \quad q \ll T/\hbar v. \tag{85}$$

Indeed, as we discussed in the previous sections the main contribution to resistivity at weak fields comes from the low energies, $\varepsilon \ll T$. Since transferred momentum $\hbar q$ is on the order of ε/v, we conclude that relevant momenta are smaller than $T/\hbar v$.

Further consideration depends on the value of the parameter $\alpha = e^2/\hbar v\varkappa$ which characterizes the strength of the electron-electron interaction. Whereas for free-standing graphene $\alpha \approx 2$, it can be much smaller for graphene grown or placed on a substrate with large dielectric constant, as well as for graphene suspended in a media with large $\varkappa$ (for example, in conventional water). Moreover, α is suppressed due to the renormalization of the Fermi velocity v.[28] Below we use α as a parameter of the theory and discuss separately two cases: $\alpha \sim 1$ and $\alpha \ll 1$.

Before going to the calculations, we note that the screening of the Coulomb impurities is not the only effect of the electron-electron interaction on transport properties of graphene. It was shown in Ref. 13 that inelastic collisions of carriers also produce a parabolic MR near the charge neutrality point. In what follows, we will first disregard inelastic collisions, taking into account only the screening effects (the role of inelastic collisions will be briefly discussed in Sec. VI). We will see that the screening of Coulomb impurities changes the situation and, remarkably, in the absence of the inelastic collisions, the low-field MR becomes proportional to $\sqrt{H}$, in a full analogy with the short-range scattering, though the temperature dependence of the MR is different.

In what follows, we focus on the contribution of the overlapping Landau levels to the MR and analyze the conductivity semiclassically within the Drude-Boltzmann approach. As we mentioned above, such approach allows one to obtain the correct equation for MR up to a numerical coefficient. For simplicity, we will consider the low-field asymptotic only.

A. Strong electron-electron interaction: $\alpha \sim 1$

In this case, for $q \ll T/\hbar v$ we find

$$V_q \approx \frac{1}{\Pi} \approx \frac{\pi\hbar^2 v^2}{NT\ln 2}. \tag{86}$$

We see that at low electron energies the scattering matrix element does not depend on the energy just as in the case of the short-range potential. Hence, in order to find low-field MR one should make the following replacement $u_0 \rightarrow u_0' = \pi\hbar^2 v^2/NT\ln 2$ and, consequently,

$$\gamma \rightarrow \gamma' = \frac{2N^2(\ln 2)^2 T^2}{n_{\rm imp}\pi^2\hbar^2 v^2}. \tag{87}$$

Since γ becomes temperature dependent we conclude that energy ε_* now also depends on T:

$$\varepsilon_* = \hbar\Omega\sqrt{\gamma'} \propto T\sqrt{H}. \tag{88}$$

Low-field MR at the Dirac point is still given by Eq. (66), where one should substitute expression (88) for ε_*. It is worth emphasizing that charged impurities yield temperature-independent MR in contrasts to inverse temperature dependence of MR in the case of short-range potential.

B. Weak electron-electron interaction: $\alpha \ll 1$.

In this case, a new energy scale αT appears within the temperature window. For small energies, $\varepsilon \ll \alpha T$, the characteristic momentum transferred in the scattering event is on the order of $\varepsilon/\hbar v$ and we get from Eq. (84): $V_q \approx 1/\Pi$. Hence, the potential is effectively short ranged and its strength is characterized by γ' [see Eq. (87)] in a full analogy with the previous subsection.

Next, we consider intermediate energies, $\alpha T \ll \varepsilon \ll T$. Analyzing Eq. (84) one might conclude that the screening can be neglected and V_q is given by its value for unscreened Coulomb potential $2\pi e^2/\kappa q$. The issue, however, is more subtle than it appears. Indeed, estimates show that the bare Coulomb potential leads to an infrared divergency of the quantum scattering rate: $1/\tau_q \sim \int_0^k dq/q^2$. This divergency is cured by screening, so that for a given electron energy ε, the characteristic value of q turns out to be much smaller than $\varepsilon/\hbar v$, being on the order of $\alpha T/\hbar v$ (see also discussion in Ref. 13). This, in turn, means that the quantum scattering rate saturates when ε becomes larger than αT. On the other hand, for $\varepsilon \gg \alpha T$ the screening can be neglected in the calculation of the transport scattering rate which is then determined by the bare Coulomb potential. As a consequence, $1/\tau_{\mathrm{tr}}$ starts to decrease as $|\varepsilon|^{-1}$ for $\varepsilon > \alpha T$.

On a more formal level, expressing the transferred momentum $q = 2(\varepsilon/\hbar v)|\sin(\theta/2)|$ through the scattering angle θ, we represent the scattering rates as

$$\frac{1}{\tau_i} \sim \alpha^2 v^2 \hbar n_{\mathrm{imp}} \varepsilon \int_0^\pi \frac{d\theta}{[\varepsilon \sin(\theta/2) + \alpha N T \ln 2]^2}$$
$$\times \begin{cases} 1 + \cos\theta, & \text{for } i = q \\ \sin^2\theta, & \text{for } i = \mathrm{tr} \end{cases}. \tag{89}$$

Evaluation of the integrals yields

$$\frac{\hbar}{\tau_q} \sim \begin{cases} \varepsilon/\gamma', & \text{for } \varepsilon \ll \alpha T; \\ \alpha T/\gamma', & \text{for } \varepsilon \gg \alpha T. \end{cases} \tag{90}$$

$$\frac{\hbar}{\tau_{\mathrm{tr}}} \sim \begin{cases} \varepsilon/2\gamma', & \text{for } \varepsilon \ll \alpha T; \\ (\alpha T)^2/\gamma'\varepsilon, & \text{for } \varepsilon \gg \alpha T. \end{cases} \tag{91}$$

Dependence of the transport and quantum scattering rates on the energy at small α is plotted schematically in Fig. 7. The value of γ' is given by Eq. (87).

Let us now consider conductivity at the Dirac point ($\mu = 0$) within the Drude-Boltzmann approach. Since most interesting results are expected at low fields, we restrict ourselves to discussion of the case $\varepsilon_* \ll \alpha T$. Using Eqs. (3), (10), and
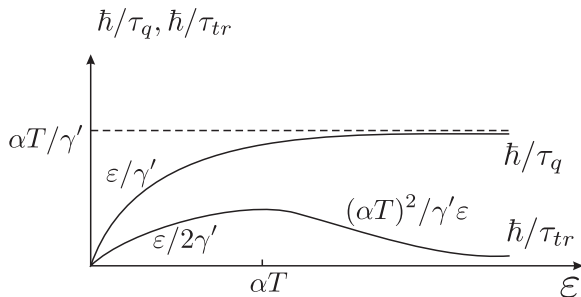

FIG. 7. Energy dependence of the quantum and transport scattering rates.

(91) we find

$$\sigma_{xx}(\varepsilon) \sim \frac{e^2 \gamma'}{\hbar} \begin{cases} \frac{\varepsilon^4}{\varepsilon^4 + \varepsilon_*^4}, & \text{for } \varepsilon \ll \alpha T; \\ \frac{\varepsilon^2 (\alpha T)^2}{(\alpha T)^4 + \varepsilon_*^4}, & \text{for } \varepsilon \gg \alpha T. \end{cases} \tag{92}$$

Next we perform the thermal averaging of $\sigma_{xx}(\varepsilon)$ and take into account that the averaged transverse conductivity at the Dirac point is zero due to the cancellation of the electron and holes contributions. Straightforward calculations yield the following result for MR:

$$\frac{\Delta \varrho_{xx}}{\varrho_{xx}(0)} \sim \begin{cases} \alpha^2 \varepsilon_*/T \propto \sqrt{H}, & \text{for } \varepsilon_* \ll \alpha^2 T; \\ (\varepsilon_*/\alpha T)^4 \propto H^2, & \text{for } \varepsilon_* \gg \alpha^2 T. \end{cases} \tag{93}$$

As seen, with increasing the magnetic field, the square-root dependence on magnetic field changes to a parabolic one. It is notable that due to the quadratic dependence of γ' on T [see Eq. (87)], the MR turns out to be temperature independent both at weak and at strong fields [see Eqs. (88) and (93)].

When deriving of Eq. (93), it was assumed that $\varepsilon^* \gg \Omega$, which implies that $\gamma' \gg 1$ [see Eq. (10)]. Actually, the latter condition is not crucial for our semiclassical treatment. Indeed, at zero field, the energy-averaged longitudinal conductivity is given by $e^2 \gamma'/\hbar \alpha^2$. This conductivity should be large compared to $e^2/\hbar$, which yields $\gamma' \gg \alpha^2$. Another condition used in the semiclassical analysis is $T\tau_q(T) \gg \hbar$. This condition, which ensures that the density of states is not changed essentially at typical energies, leads to a stronger inequality [see Eq. (90)]: $\gamma' \gg \alpha$. Hence, in contrast to the case of short-range disorder, γ' can be smaller than unity. For $\alpha \ll \gamma' \ll 1$, the MR is parabolic and is given by the bottom line of Eq. (93) in the whole range of magnetic fields addressed in the paper.

Finally we note that the potential of the charged impurities is also screened by the gate electrode. Such screening becomes important at low temperatures, when characteristic values of the transferred momentum, $q \sim T/\hbar v$, become smaller than the inverse spacer distance, $1/d$. In this case, the amplitude of the screened impurity potential is estimated as $V_q = 2\pi e^2 d/\varkappa = \text{const}$, so that this case is equivalent to the case of the short-range disorder.

VI. ROLE OF INELASTIC COLLISIONS

So far we have completely disregarded the effect of inelastic collisions induced by Coulomb interaction between the carriers. In fact, such collisions are crucially important for transport properties of clean graphene in the vicinity of the Dirac point ($\mu \ll T$).[13,25,26,31–35] A detailed analysis of the MR in the presence of such collisions is out of the scope of the current research. Here we limit ourselves to a qualitative discussion of the problem.

Let us first return to the case of short-range impurity potential. For electrons with typical energies, $\varepsilon \sim T$, the rate of inelastic collisions is of the order of $1/\tau_{ee} \sim \alpha^2 T/\hbar$. This rate should be compared with the characteristic scattering rate off impurities [see Eq. (7)], which yields for typical energies $\varepsilon \sim T$: $1/\tau_q \sim 1/\tau_{\mathrm{tr}} \sim T/\gamma\hbar$. Since γ is large by assumption, the existence of the disorder-dominated regime requires rather

weak interaction:

$$\alpha^2 \ll 1/\gamma \ll 1. \tag{94}$$

In the opposite limit, $\alpha^2 \gg 1/\gamma$, the hydrodynamic approach developed in Ref. 13 yields a parabolic MR. As we already mentioned above, the interaction constant $\alpha = e^2/\hbar v \varkappa$ can be much smaller than unity for graphene grown on a substrate with large dielectric constant or for graphene suspended in a media with large $\varkappa$. Furthermore, α is suppressed due to the renormalization of the Fermi velocity v.[28] This implies that inequality $\alpha^2 \ll 1/\gamma$ can be satisfied in experiments.

We now briefly discuss the competition between the scattering off the charged impurities and the electron-electron collisions. As follows from Eq. (91), for typical energies, $\varepsilon \sim T$, scattering rate is estimated as $1/\tau_{\rm tr} \sim \alpha^2 T/\hbar \gamma'$. Comparing this rate with the inelastic one, $1/\tau_{ee}$, we arrive at the conclusion that at $\gamma' \gg 1$ the electron-electron collisions dominate over the impurity scattering. In this case, the MR is parabolic and described by the theory developed in Ref. 13. In the notation used above, one can represent MR obtained in Ref. 13 for the case $\mu = 0$ as follows:

$$\frac{\Delta \varrho_{xx}}{\varrho_{xx}(0)} \sim \omega_c(T)^2 \tau_{ee}(T) \tau_{\rm tr}(T) \sim \left(\frac{\varepsilon_*}{\alpha T}\right)^4 \frac{1}{\gamma'}. \tag{95}$$

We see that in the collision-dominated regime, inelastic collisions suppress the MR by a factor of $\gamma' \gg 1$ as compared to the collisionless case [see the bottom line in Eq. (93)].

In the opposite limit, $\gamma' \ll 1$, the scattering by impurities dominates over the electron-electron collisions. Nevertheless, the low-field asymptotic of MR [the top line of Eq. (93)] is not realized. Indeed, the condition $\epsilon \tau_q/\hbar \gg 1$, which ensures that the spectrum is not essentially affected by scattering, is equivalent to the condition $\varepsilon \gg \alpha T/\gamma'$ and, therefore, is not satisfied in the region of relevant energies, $\varepsilon \sim \varepsilon_* \ll \alpha^2 T$. However, at high fields, the MR is dominated by impurity scattering and is given by the bottom line of Eq. (93) provided that $\gamma' \gg \alpha$ (as we mentioned above, the latter condition ensures that the spectrum is not changed at typical energies $\varepsilon \sim T$).

Let us finally emphasize that the square-root low-field MR due to the scattering off Coulomb impurities can be obtained in the gated graphene. The gate screens the Coulomb potential, thus weakening both the impurity and the electron-electron scattering. Here we focus on the case of low temperatures $T \ll \hbar v/d$, when for typical energies ($\varepsilon \sim T$) and wave vectors ($q \sim T/\hbar v$) we get $V_q \sim e^2 d/\varkappa$ and, consequently, find

$$\frac{1}{\tau_q} \sim \frac{1}{\tau_{\rm tr}} \sim \frac{T}{\hbar \gamma''}, \tag{96}$$

$$\gamma'' \sim \frac{\hbar^2 v^2}{n_{\rm imp} V_q^2} \sim \frac{1}{\alpha^2 n_{\rm imp} d^2}, \tag{97}$$

$$\frac{1}{\tau_{ee}} \sim \frac{\alpha^2 T}{\hbar} \left(\frac{Td}{\hbar v}\right)^2. \tag{98}$$

Condition $\gamma'' \gg 1$ yields

$$n_{\rm imp} \ll \frac{1}{\alpha^2 d^2}. \tag{99}$$

Impurity scattering dominates over electron-electron collisions when $1/\tau_{\rm tr} \gg 1/\tau_{ee}$, thus giving another restriction,

$$T \ll \hbar v \sqrt{n_{\rm imp}}. \tag{100}$$

It is easy to see that both inequalities, Eq. (99) and (100), can be satisfied in the limit of low temperatures for sufficiently low concentration of impurities. At such concentrations and temperatures, the MR is given by expressions derived above for the short-range disorder with the replacement of γ by γ''.

It is worth noticing that the assumption about the absence of Shubnikov–de Haas oscillations limits possible temperatures from below: $T \gg \hbar \Omega/\sqrt{\gamma''}$. In combination with Eq. (100), this condition yields a parametrically large range of temperatures for the square-root MR, provided that $\alpha d/l_H \ll 1$. Thus we conclude, that the low-field square-root MR is a generic feature in a realistic gated setup in a wide range of experimentally accessible parameters.

Above we presented estimates both for short-range disorder and for charged impurities assuming that the electron energies are on the order of T. In fact, the situation is more complicated because the main contribution to the square-root dependence obtained above comes from small (untypical) energies ($\varepsilon \ll T$). The analysis of electron-electron collisions for such energies is nontrivial and should take into account the plasmon-assisted scattering mechanism[25] (though the plasmons are not important[25,31,32] for those transport properties that are determined by energies on the order of T). The MR in the presence of interaction might still be determined by low untypical energies. Detailed study of the plasmon-assisted scattering and its competition with the impurity scattering is a challenging problem which will be discussed elsewhere.

VII. DISCUSSION AND CONCLUSIONS

To conclude, we have studied magnetotransport in graphene, focusing on the case of short-range disorder. We have found that MR depends on three relevant parameters having dimensionality of the energy, μ, T, and ε_*, the field dependence being fully absorbed by ε_* which is proportional to $\sqrt{H}$. One of the main predictions of our model is the square-root field dependence of MR in the limit of low H, both at very low and at very high temperatures. Such a dependence persists down to exponentially small fields, corresponding to $\varepsilon_* \sim \Delta e^{-\pi \gamma/2}$.

We separately analyzed the cases of low and high temperatures and identified four different transport regimes for $\mu \gg T$ and three regimes for $\mu \ll T$ (see Fig. 4). All these regimes can be realized provided that temperature lays within a certain interval. Let us now find the corresponding criteria.

For $\mu \gg T$ and not too small ε_*, MR is determined by energies close to the Fermi surface, $\varepsilon \approx \mu$. Above we assumed that Shubnikov-de Haas oscillations are suppressed by energy averaging within the temperature window, which implies that $T \gg \hbar \omega_c(\mu)$. Using Eqs. (3) and (10), the latter inequality can be rewritten as $\varepsilon_* \ll \sqrt{\gamma T \mu}$. While identifying regimes shown at the upper picture in the Fig. 4 we implicitly assumed that $\sqrt{\gamma T \mu}$ is larger than μ, or, equivalently, $T > \mu/\gamma$. When T becomes smaller than μ/γ the high-field square-root asymptotic of MR is not realized because of arising of Shubnikov de Haas oscillations at $\varepsilon_* \sim \sqrt{\gamma T \mu} \ll \mu$. However, the low-field

square-root asymptotic is determined by energies $\varepsilon \sim \varepsilon_*$ and remains valid even at low temperature, because Eq. (12) is always satisfied for $T \ll \mu$ and $\varepsilon_* < \varepsilon_2$.

In the opposite limiting case, $T \gg \mu$, the main contribution to MR comes from $\varepsilon \approx \varepsilon_*$. Rewriting Eq. (12) as $\varepsilon_* \ll \gamma T$, we find that three regimes shown in Fig. 4 are realized provided that $\gamma T \gg T^2/\mu$, or, equivalently, $T \ll \gamma \mu$. At higher temperatures, $T \gg \gamma \mu$, MR is given by $C_3 \varepsilon_*/2T$ for $\varepsilon_* \ll T$ and $C_4(\varepsilon_*/T)^3$ in the interval $T \ll \varepsilon_* \ll \gamma T$. The Shubnikov–de Haas oscillations appear at $\varepsilon_* \gg \gamma T$.

We predicted a nontrivial behavior of the Hall coefficient on H in the vicinity of the Dirac point. With increasing the field, R decreases, reaches a minimum and then starts to grow again. Furthermore, we analyzed dependence of R on electron concentration and found that this dependence is nonmonotonic both for law and strong fields.

We also estimated the MR caused by scattering off the charged, partially screened impurities and discussed the competition between disorder- and collision-dominated mechanisms of MR. Importantly, the main prediction of our theory, the square-root dependence of MR in the limit of weak fields, is also valid at sufficiently low temperatures in the case of charged impurity potential when the screening by an external gate is taken into account. Specifically, in this situation, the range of T, where the effect takes place, is parametrically large for $\alpha d/l_H \ll 1$ which is easily accessible in experiments.

Before concluding the paper, let us discuss some interesting problems to be addressed in future. First, we note that our theory is applicable to any other 2D electron systems with the linear energy spectrum. Simplest examples are surfaces of three-dimensional (3D) topological insulators and 2D spin-orbit metals based, in particular, on the CdTe/HgTe quantum wells with the chemical potential moved away from the gap.[29,30] The latter example needs some comments. The energy spectrum in 2D spin-orbit metals is not purely linear (with the only exception for a certain width of the quantum well), so that the evident generalization of our theory is the calculation of the MR for the case of a small but finite effective mass m of the carriers. Besides 2D spin-orbit metals, such a

theory would apply to a bilayer graphene. We expect that for a quasilinear spectrum, MR would depend on the relation between T and mv^2. In the most interesting case, $\mu \ll T$, we expect parabolic MR at $T \ll mv^2$ which would cross over to the square-root MR at $T \gg mv^2$. Furthermore, our work motivates the following question related to the interaction effects in graphene: What is the effect of inelastic scattering (including the role of plasmons) on the Landau-level broadening in graphene? In particular, in a clean sample, Coulomb interaction is the only source of such broadening (note that it is this broadening that justifies a semiclassical hydrodynamic approach). A square-root MR might still arise in the presence of inelastic scattering in graphene for sufficiently strong magnetic fields, such that within the temperature window both regions of separated and overlapping Landau levels are present, as in the disorder-dominated regime addressed in our work. Finally, it is interesting to analyze the MR of a suspended graphene, where scattering by flexural phonons is crucially important for the transport properties.[36]

Note added. After this work was completed, the experimental evidence of square-root MR in monolayer graphene was reported.[37] Furthermore, very recently, the ac magnetoconductivity was calculated in Ref. 38 for the case of pointlike impurities in graphene; the results of Ref. 38 in the limit $\omega \to 0$ are in agreement with our predictions.

[1] T. Ando, Rev. Mod. Phys. **54**, 437 (1982).

[2] S. D. Sarma, S. Adam, E. H. Hwang, and E. Rossi, Rev. Mod. Phys. **83**, 407 (2011).

[3] T. Ando and Y. Uemura, Journ. of the Phys. Soc. of Japan **36**, 959 (1974).

[4] T. Ando, Journ. of the Phys. Soc. of Japan **36**, 1521 (1974).

[5] T. Ando, Journ. of the Phys. Soc. of Japan **37**, 622 (1974).

[6] T. Ando, Journ. of the Phys. Soc. of Japan **37**, 1233 (1974).

[7] N. H. Shon and T. Ando, Journ. of the Phys. Soc. of Japan **67**, 2421 (1998).

[8] Y. Zheng and T. Ando, Phys. Rev. B **65**, 245420 (2002).

[9] V. P. Gusynin and S. G. Sharapov, Phys. Rev. B **71**, 125124 (2005); **73**, 245411 (2006).

[10] N. M. R. Peres, F. Guinea, and A. H. Castro Neto, Phys. Rev. B **73**, 125411 (2006).

[11] B. Dora and P. Thalmeier, Phys. Rev. B **76**, 035402 (2007).

[12] P. M. Ostrovsky, I. V. Gornyi, and A. D. Mirlin, Phys. Rev. B **77**, 195430 (2008).

[13] M. Müller, L. Fritz, and S. Sachdev, Phys. Rev. B **78**, 115406 (2008); M. Müller and S. Sachdev, *ibid.* **78**, 115419 (2008); M. Müller, L. Fritz, S. Sachdev, and J. Schmalian, AIP Conf. Proc. **1134**, 170 (2009).

[14] J. Jobst, D. Waldmann, I. V. Gornyi, A. D. Mirlin, and H. B. Weber, Phys. Rev. Lett. **108**, 106601 (2012).

[15] A. H. Castro Neto, F. Guinea, N. M. R. Peres, K. S. Novoselov, and A. K. Geim, Rev. Mod. Phys. **81**, 109 (2009).

[16] T. Ando and T. Nakanishi, Journ. of the Phys. Soc. of Japan **67**, 1704 (1998).

[17] P. M. Ostrovsky, I. V. Gornyi, and A. D. Mirlin, Phys. Rev. B **74**, 235443 (2006).

[18]The factor μ/T in the averaged value of σ_{xy}^{D} appeared due to the partial cancellation of the electron and hole contributions which have different signs. This factor is absent in an artificial model where there is only one sort of Dirac carriers (say, electrons). It is worth noting that even in this model, the averaged transverse conductivity, $\sigma_{xy}^{D} \sim |\Delta\sigma_{xx}(H)|$, satisfies Eq. (21) and the estimate (23) holds, giving rise to a square-root MR.

[19]I. A. Dmitriev, A. D. Mirlin, D. G. Polyakov, and M. A. Zudov, Rev. Mod. Phys. **84**, 1709 (2012).

[20]T. Ando, Y. Matsumoto, and Y. Uemura, Journ. of the Phys. Soc. of Japan **39**, 279 (1975).

[21]P. Streda, J. Phys. C **15**, L717 (1982).

[22]M. G. Vavilov and I. L. Aleiner, Phys. Rev. B **69**, 035303 (2004).

[23]Within the SCBA, the transverse conductivity including both $\sigma_{xy}^{I}(\varepsilon)$ and $\sigma_{xy}^{II}(\varepsilon)$ can be written as follows:[20]

$$\sigma_{xy}(\varepsilon) = \frac{ecn(\varepsilon,H)}{H} - \frac{\sigma_{xx}(\varepsilon)z(\varepsilon)}{\omega_{c}(\varepsilon)\tau_{\mathrm{tr}}(\varepsilon)}.$$

This equation is obtained from the semiclassical Drude-Boltzmann relation between $\sigma_{xx}(\varepsilon)$ and $\sigma_{xy}(\varepsilon)$ by replacement of τ_{tr} with τ_{tr}/z. Subtracting $\sigma_{xy}^{I}(\varepsilon)$ [given by Eq. (43)] from this relation, one finds a convenient representation for thermodynamical contribution to the Hall conductivity,

$$\sigma_{xy}^{II}(\varepsilon) = \frac{e^{2}N}{2\pi\hbar^{3}\Omega^{2}}\left[\int_{0}^{\varepsilon} z(\varepsilon')|\varepsilon'|d\varepsilon' - \frac{|\varepsilon|\varepsilon z(\varepsilon)}{2}\right].$$

Averaging the latter equation over energy within the interval $\delta\varepsilon$ one finds that the thermodynamical contribution can be neglected.

[24]In the energy range $\varepsilon \gg \varepsilon_{*}$ corresponding to overlapping Landau levels, $\sigma_{xy}^{II}(\varepsilon)$ is exponentially small and besides that is an oscillatory function of energy, whereas the exponentially small correction to $\sigma_{xy}^{I}(\varepsilon)$ contains a nonoscillatory term. Therefore, energy-averaged contribution to the transverse conductivity, $\bar{\sigma}_{xy}^{II}(\varepsilon)$, is smaller than the exponential correction to $\bar{\sigma}_{xy}^{I}(\varepsilon)$.

[25]M. Schütt, P. M. Ostrovsky, I. V. Gornyi, and A. D. Mirlin, Phys. Rev. B **83**, 155441 (2011).

[26]B. N. Narozhny, M. Titov, I. V. Gornyi, and P. M. Ostrovsky, Phys. Rev. B **85**, 195421 (2012); M. Schütt, P. M. Ostrovsky, M. Titov, I. V. Gornyi, B. N. Narozhny, and A. D. Mirlin, Phys. Rev. Lett. **110**, 026601 (2013).

[27]One can show that crossover from Eq. (80) to Eq. (73) happens in the interval of concentration corresponding to $T < \mu < T\ln[\ln(T/\varepsilon_{*})]$.

[28]J. González, F. Guinea, and M. A. H. Vozmediano, Nucl. Phys. B **424**, 595 (1994); Phys. Rev. B **59**, R2474 (1999).

[29]M. Z. Hasan and C. L. Kane, Rev. Mod. Phys. **82**, 3045 (2010).

[30]X.-L. Qi and S.-C. Zhang, Rev. Mod. Phys. **83**, 1057 (2011).

[31]A. B. Kashuba, Phys. Rev. B **78**, 085415 (2008).

[32]L. Fritz, J. Schmalian, M. Müller, and S. Sachdev, Phys. Rev. B **78**, 085416 (2008).

[33]M. S. Foster and I. L. Aleiner, Phys. Rev. B **77**, 195413 (2008).

[34]M. Müller, J. Schmalian, and L. Fritz, Phys. Rev. Lett. **103**, 025301 (2009).

[35]M. S. Foster and I. L. Aleiner, Phys. Rev. B **79**, 085415 (2009).

[36]See I. V. Gornyi, V. Yu. Kachorovskii, and A. D. Mirlin, Phys. Rev. B **86**, 165413 (2012), and references therein.

[37]G. Yu. Vasil'eva, P. S. Alekseev, Yu. L. Ivanov, Yu. B. Vasil'ev, D. Smirnov, H. Schmidt, R. J. Haug, F. Gouider, and G. Nachtwei, Pis'ma v ZhETP **96**, 519 (2012) [JETP Lett. **96**, 471 (2012)].

[38]U. Briskot, I. A. Dmitriev, and A. D. Mirlin, arXiv:1301.7246.